IJNAOE
©SNAK, 2015

Int. J. Nav. Archit. Ocean Eng. (2015) 7:526~539
http://dx.doi.org/10.1515/ijnaoe-2015-0038
pISSN: 2092-6782, eISSN: 2092-6790

Underwater striling engine design with modified one-dimensional model

Daijin Li[1], Kan Qin[2] and Kai Luo[1]

[1]*School of Marine Science and Technology, Northwestern Polytechnical University, Xi'an, China*
[2]*School of Mechanical and Mining Engineering, University of Queensland, Australia*

Received 9 September 2014; Revised 27 November 2014; Accepted 24 March 2015

ABSTRACT: *Stirling engines are regarded as an efficient and promising power system for underwater devices. Currently, many researches on one-dimensional model is used to evaluate thermodynamic performance of Stirling engine, but in which there are still some aspects which cannot be modeled with proper mathematical models such as mechanical loss or auxiliary power. In this paper, a four-cylinder double-acting Stirling engine for Unmanned Underwater Vehicles (UUVs) is discussed. And a one-dimensional model incorporated with empirical equations of mechanical loss and auxiliary power obtained from experiments is derived while referring to the Stirling engine computer model of National Aeronautics and Space Administration (NASA). The P-40 Stirling engine with sufficient testing results from NASA is utilized to validate the accuracy of this one-dimensional model. It shows that the maximum error of output power of theoretical analysis results is less than 18% over testing results, and the maximum error of input power is no more than 9%. Finally, a Stirling engine for UUVs is designed with Schmidt analysis method and the modified one-dimensional model, and the results indicate this designed engine is capable of showing desired output power.*

KEY WORDS: Stirling engine; Unmanned underwater vehicles (UUVs); One-dimensional model; Thermodynamic performance.

NOMENCLATURE

M	mass of working fluid, [kg]	C_v	specific heat at constant volume, [$J/kg \cdot K$]
P	pressure of working space, [Pa]	h	heat transfer coefficient, [$W/m^2 \cdot K$]
V	volume, [m^3]	A	heat transfer area, [m^2]
T	temperature, [K]	R	gas constant, [$J/kg \cdot K$]
W	mass flow rate, [kg/s]	Z	compressibility factor, [-]
Q	heat transfer, [W]	W_{ml}	mechanical loss, [kW]
$work$	work, [W]	n	engine speed, [rpm]
C_p	specific heat at constant pressure, [$J/kg \cdot K$]	p_m	mean pressure, [MPa]

Corresponding author: *Daijin Li*, e-mail: *lidaijin@nwpu.edu.cn*

P_{in}	indicated power, [W]	Nu	nusselt number, [-]
P_{out}	output power, [W]	Re	reynolds number, [-]
W_{aux}	auxiliary power, [kW]	φ	phase angle, [*rad*]
t	time, [sec]	α	crank angle, [*rad*]
Δt	time interval, [sec]		

SUBSCRIPTS

w	wall	*	interface
d	design point	s	updated value for the change in specific heat
i	index of CV	sp	updated value for the change in specific heat and pressure
in	inlet	spm	updated value for the change in specific heat and pressure, and mass mixture
out	outlet		
e	expansion space		
c	compression space		

INTRODUCTION

Under the circumstance of limited space for underwater power system, Stirling engines are regarded as an efficient and promising power system for UUVs due to the advantages of compactness, high efficiency and ability to use various heat sources (Wang et al., 2012; Shih et al., 2013). Most importantly, the Stirling engine is an external combustion engine, and thus various types of heat sources can be utilized, including solar energy (Mancini et al., 2003; Kongtragool and Wongwises, 2003; Tlili et al., 2008; Abdullah et al., 2005), waste heat (Shoureshi, 1978; Li et al., 2012; Cullen and McGovern, 2010), or biomass (Waters, 2013). Reader (Reader, 1998) stated that Stirling engines were particularly attractive for marine applications. Mattavi et al. (1969) at General Motors presented basic description of some Stirling engines along with complete maps of performance data and other facts related to their underwater use with closed energy sources, and predicted performance characteristics for power-plant systems combining Stirling engines with heat storage and metal-combustion energy sources. Nilsson (Nilsson, 1983) presented that the United Stirling 4-95 and 4-275 well-known engines had been adapted to underwater operation. Swedish shipbuilder Kockums had built 8 successful Stirling powered submarines since the late 1980s, which were the first submarines in the world to feature Stirling air-independent propulsion, and extended their underwater endurance from a few days to several weeks.

Even though Stirling engines have shown great advantages in underwater environment, the present applications of the Stirling engine to underwater devices only specify to the submarine. To the knowledge of the author, there are few studies about Stirling engines applied to UUV, Bratt (1990) pointed out that Kockums Marine had developed a prototype energy system based on the 4-95 engine for use in an UUV, which coupled with a combustor that burns diesel fuel oxygen. Reader et al. (1998) described the application of the Stirling engine for underwater duties, and in particular the selection, design and development of a Stirling engine powered Drive Propulsion Vehicle (DPV).

Also, during the last several decades, a large number of studies have been done on the development of theoretical methods for the analysis of the thermodynamic performance of different types of Stirling engines, for the use in the design stage and for the prediction of their performance. Various models have been developed and are used for the simulation of the thermodynamic performance of Stirling engines.

Zeroth order analysis

Beale (1969) observed that most modern engines operate under similar conditions of the parametric ratio: dead volume ratio, temperature ratio, swept volume ratio, displacer-piston phase angle advance, and he presented that engine performance could be represented in terms of mean pressure, swept volume and operational frequency.

First order analysis

The first order analysis of Stirling engines was done by Schmidt (Schmidt, 1871), he obtained closed-form solutions for the special case of sinusoidal volume variations and isothermal hot and cold spaces, however, it does not take into account non-isothermal effects and internal irreversibility caused by fluid friction and the pressure difference in different spaces of the engine.

Second order analysis

The second order analysis model is based on an adiabatic analysis that subtracts losses caused by heat transfer and flow power losses. It relies on a modified Schmidt analysis and requires nonlinear time integration of ordinary differential equations. Urieli and Berchowitz (1984) had given a detailed description of it. Based on the thoughts of adiabatic analysis, Tilli et al. (2008; 2013) and Timoumi et al. (2008a; 2008b) proposed an alternative adiabatic analysis model, which divided the regenerator into two parts, this model was used to determine losses in different engine compartments and to calculate the geometrical and physical parameters corresponding to minimal losses.

Third order analysis

In the third order analysis model, the thermodynamic performance of the engine is described by the set of partial differential equations of mass, momentum, and energy conservation, and equations of state. Some of the first analysis at this level of fidelity was accomplished by Finkelstein (Finkelstein, 1960). However, these equations usually do not take into account any influence of the turbulence in the flow.

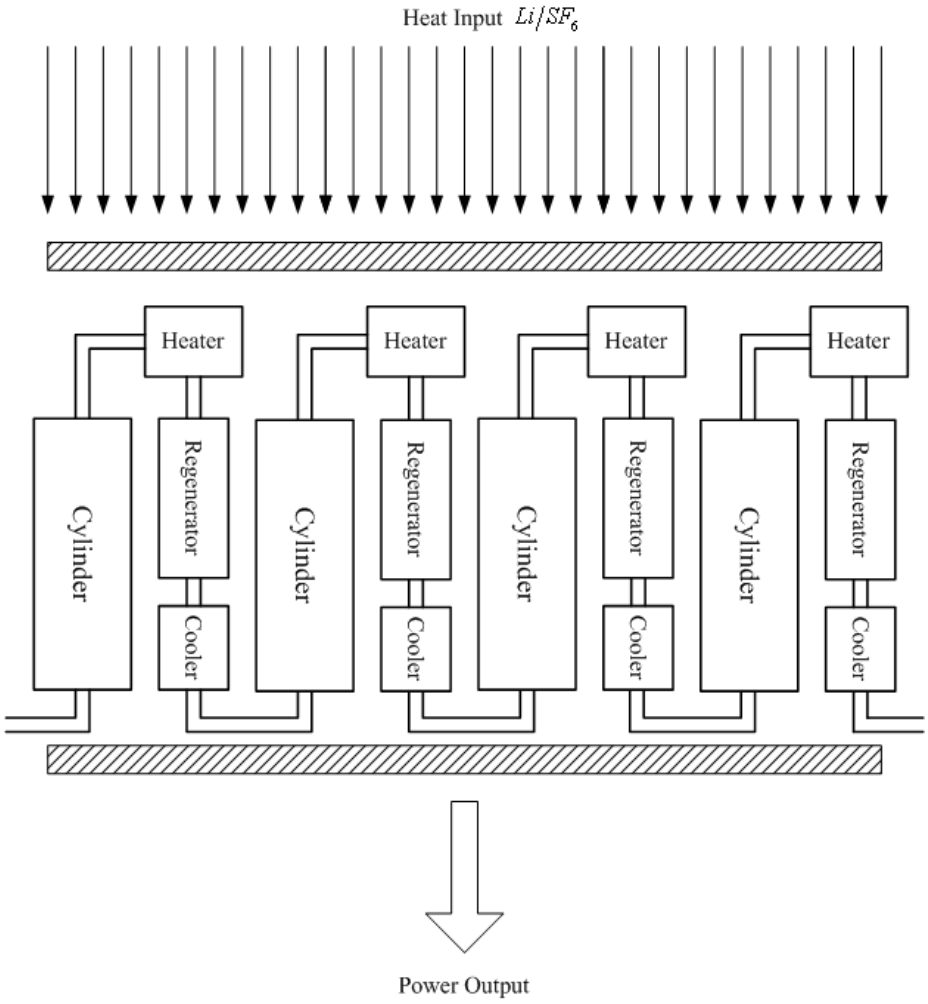

Fig. 1 Schematic diagram of the Stirling engine system for UUVs.

Fourth order analysis

Little research has been accomplished (Mahkamov, 2006; Tew et al., 1978) to study this level of analysis, since the third order analysis is faster and an adequate engineering tool. However, to understand and reduce losses, it will likely require a better understanding of the actual flow features and heat transfer throughout the engine.

Under these circumstances, this study is aimed to develop a Stirling engine system for UUV, which is able to efficiently work in the underwater environment of limited space, and then the Stirling engine for UUV is investigated.

SYSTEM CONFIGURATIONS

In order to improve the efficiency of power system with high energy density of Li/SF_6, the engine technology might be an alternative solution to meet the mission requirements of a typical UUV. And alpha engine can be compounded into a more compact multiple cylinder configuration. Usually a four-cylinder engine is adopted for supplying a high specific power output, the four cylinders are interconnected, and the expansion space of one cylinder is connected to the compression space of the adjacent cylinder via a series of heater, regenerator and cooler, this special configuration shows great advantage of compactness over other engines. Hence, the schematic diagram of the Stirling engine system for UUV is shown in Fig. 1 where the combination of Li/SF_6 provides heat to the Stirling engine, and a four-cylinder double-acting Stirling engine is used to convert heat to mechanical power.

MATHEMATICAL MODEL

One-dimensional model

In order to evaluate the thermodynamic performance of a Stirling engine, a modified third order analysis model combining with empirical equations obtained from experiments should be presented, and is called as one-dimensional model.

The one-dimensional model would require the solution of a set of partial differential equations. The simulation problem can be simplified by assuming the flow is one-dimensional and dividing the working space into a number of Control Volumes (CVs). A set of partial differential equations is then solved for each CV, and the assumptions made in this analysis are expressed as follows.

- The instantaneous pressure is uniform throughout the Stirling engine and the pressure drop along the Stirling engine is neglected.
- Heat transfer in the heat exchangers, i.e., the heater, the cooler and the regenerator, are evaluated using empirical equations under steady flow condition.
- No leakage is allowed either through the appendix gap or through the seals of the connecting rods.

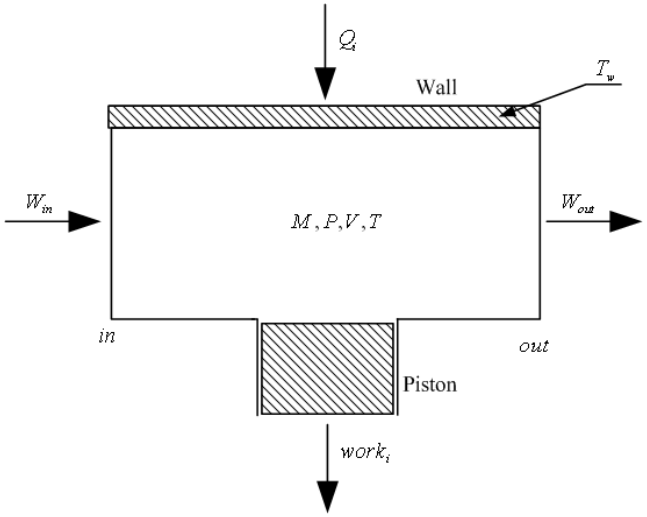

Fig. 2 Generic CV.

The pressure drop in the engine is the summation of the pressure drops in the cooler, regenerator and heater. Since in most high pressure Stirling engines, the pressure swing is usually a small fraction of the charge pressure, typically less than 15%, if the variation of density with pressure is neglected (Rogdakis et al., 2004). During the preliminary design stage, the instantaneous pressure is uniform throughout the Stirling engine and the pressure drop along the Stirling engine is neglected.

The schematic diagram of the generic CV used in the thermodynamic analysis of Stirling engines is shown in Fig. 2. The generic CV includes mass flowing across control boundary, heat transfer through the wall, and work interchange between the working fluid and the piston, and other CVs can be regarded as a special case of this generic CV. Only the volumes of expansion space and compression space are variable while the others remain constant.

The fundamental equations used to model the thermodynamics performance of the Stirling engine in each CV are mass conservation, energy conservation, momentum conservation, and Equations of State (EoS). Since pressure drop along the CV is neglected, momentum conservation is not considered here. These equations are used to determine temperature, pressure, mass and other variables within each CV at a particular time. The energy conservation for the generic CV shown in Fig. 2 can be summarized as follows:

$$\frac{d}{dt}\left(MC_vT\right) = hA\left(T_w - T\right) + \left(C_{p,in}W_{in}T_{in} - C_{p,out}W_{out}T_{out}\right) - P\frac{dV}{dt} \tag{1}$$

The mass conservation is expressed as:

$$\frac{dM}{dt} = W_{in} - W_{out} \tag{2}$$

Generally, the thermophysical properties of the working fluid in Stirling engines are assumed as ideal gas (Tew et al., 1978), however, the working fluid cannot be simply taken as ideal gas, but dense gas in the Stirling engine, i.e., dense gases are usually defined as single-phase vapors whose thermodynamic state is close to saturation conditions, at temperatures and pressures of the order of magnitude of the critical ones. Under this dense gas region, real gas effects play a crucial role in the dynamic behavior of the working fluid. Angelino and Invernizzi (2010) studied the real gas effect on the performance of the Stirling engine, and concluded that real gas effects in the working fluid critical region was shown to be a powerful tool to increase the energy conversion efficiency of Stirling cycles, mainly at low top temperatures. There are several types of real gas models, namely, van der waals EoS, Peng-Robinson Eos, Redlich-Kwong EoS or multiparameter EoS. In this paper, to simplify the computational process, a compressibility factor Z is added to ideal equations of state, and the value of this compressibility factor Z could be determined by considering the mean working condition of the Stirling engine, then the equation of state for real gas is written as:

$$PV = ZMRT \tag{3}$$

Expanding the first term of Eq. (1) then gives:

$$MC_v\frac{dT}{dt} + C_vT\frac{dM}{dt} + MT\frac{dC_v}{dt} = hA\left(T_w - T\right) + \left(C_{p,in}W_{in}T_{in} - C_{p,out}W_{out}T_{out}\right) - P\frac{dV}{dt} \tag{4}$$

Differentiating Eq. (3) yields:

$$Z\left(MR\frac{dT}{dt} + RT\frac{dM}{dt}\right) = P\frac{dV}{dt} + V\frac{dP}{dt} \tag{5}$$

Letting $R = C_p - C_v$ and Eq. (5) can be expressed as

$$ZC_vT\frac{dM}{dt} = ZM\left(C_p - C_v\right)\frac{dT}{dt} + ZC_pT\frac{dM}{dt} - P\frac{dV}{dt} - V\frac{dP}{dt} \tag{6}$$

Substituting the right side of Eq. (6) with Eq. (4) then yields:

$$\begin{aligned} &M\left(ZC_p - ZC_v + C_v\right)\frac{dT}{dt} + T\left(ZC_p - ZC_v + C_v\right)\frac{dM}{dt} - V\frac{dP}{dt} + MT\frac{dC_v}{dt} \\ &= hA\left(T_w - T\right) + \left(C_{p,in}W_{in}T_{in} - C_{p,out}W_{out}T_{out}\right) \end{aligned} \tag{7}$$

Because $\frac{dC_v}{dt} = \frac{dC_p}{dt}$, Eq. (7) then can be expressed as follows:

$$\begin{aligned} \frac{dT}{dt} &= \frac{hA}{M\left(ZC_p - ZC_v + C_v\right)}\left(T_w - T\right) + \frac{T\left(W_{out} - W_{in}\right)}{M} + \frac{\left(C_{p,in}W_{in}T_{in} - C_{p,out}W_{out}T_{out}\right)}{M\left(ZC_p - ZC_v + C_v\right)} \\ &+ \frac{V}{M\left(ZC_p - ZC_v + C_v\right)}\frac{dP}{dt} - \frac{T}{\left(ZC_p - ZC_v + C_v\right)}\frac{dC_p}{dt} \end{aligned} \tag{8}$$

It is shown in Eq. (8) that the variation of the temperature in each CV is mainly influenced by four factors, i.e., heat transfer, mass mix, the change of pressure and the change of specific heat at constant pressure. The approach used in numerically integrating Eq. (8) is to decouple the four influence factors that contribute to the temperature change and solve the temperature variation due to each factor individually (Tew et al., 1978). The temperature variation is represented by following forms:

$$\frac{dT}{dt} = -\frac{T}{\left(ZC_p - ZC_v + C_v\right)}\frac{dC_p}{dt} \tag{9}$$

$$\frac{dT}{dt} = \frac{V}{M\left(ZC_p - ZC_v + C_v\right)}\frac{dP}{dt} \tag{10}$$

$$\frac{dT}{dt} = \frac{T\left(W_{out} - W_{in}\right)}{M} + \frac{\left(C_{p,in}W_{in}T_{in} - C_{p,out}W_{out}T_{out}\right)}{M\left(ZC_p - ZC_v + C_v\right)} \tag{11}$$

$$\frac{dT}{dt} = \frac{hA}{M\left(ZC_p - ZC_v + C_v\right)}\left(T_w - T\right) \tag{12}$$

Eqs. (9), (10) and (12) can be integrated in a closed form and equation (11) can be numerically integrated, therefore, the discrete expressions are written as:

$$T_s^{t+\Delta t} = T^t\left(\frac{ZC_p^t - ZC_v^t + C_v^t}{ZC_p^{t+\Delta t} - ZC_v^{t+\Delta t} + C_v^{t+\Delta t}}\right)^{\frac{1}{Z}} \tag{13}$$

$$T_{sp}^{t+\Delta t} = T_s^{t+\Delta t}\left(\frac{p^{t+\Delta t}}{p^t}\right)^{\frac{ZR}{ZC_p^{t+\Delta t} - ZC_v^{t+\Delta t} + C_v^{t+\Delta t}}} \tag{14}$$

$$T_{spm}^{t+\Delta t} = \frac{M^t}{M^{t+\Delta t}} T_{sp}^{t+\Delta t} + \frac{\left(C_{p,in}^{t+\Delta t} W_{in}^{t+\Delta t} T_{in}^{t+\Delta t} - C_{p,out}^{t+\Delta t} W_{out}^{t+\Delta t} T_{out}^{t+\Delta t}\right)}{M^{t+\Delta t}\left(ZC_p^{t+\Delta t} - ZC_v^{t+\Delta t} + C_v^{t+\Delta t}\right)}\Delta t \tag{15}$$

$$T^{t+\Delta t} = T_{spm}^{t+\Delta t} - \left(T_w - T_{spm}^{t+\Delta t}\right)\left(1 - e^{-\frac{hA}{M\left(ZC_p^{t+\Delta t} - ZC_v^{t+\Delta t} + C_v^{t+\Delta t}\right)}\Delta t}\right) \tag{16}$$

Eq. (13) denotes the updated value of the temperature for the influence of change in specific heat, Eq. (14) denotes the updated value of the temperature for the influence of change in specific heat and pressure, Eq. (15) denotes the updated value of the temperature for the influence of specific heat, pressure and mass mixture, and Eq. (16) denotes the value of the temperature after it has been updated for all four influence factors.

Interface temperature and heat transfer coefficient

Generally, the interface temperature can be regarded as the temperature of adjacent CVs along with the mass flow direction, or up-wind scheme, which can be written as:

$$\begin{cases} T_i^* = T_{i-1} & W_i \geq 0 \\ T_i^* = T_i & W_i < 0 \end{cases} \tag{17}$$

This assumption is reasonable since the temperature gradient across each CV in the heater or cooler is relatively small. In the regenerator, however, the temperature gradient is not comparatively small, and the common solution is to increase the number of CVs in the regenerator. However, in order to save computing time, an alternative approach was used (Tew et al., 1978). The schematic diagram of CV and temperature distribution in the regenerator is shown in Fig. 3. The cross-hatched area represents the portion of the working fluid that will flow across interface i during the time step Δt. For the flow direction shown in Fig. 3, the temperature of the working fluid that crosses the interfaces during the time Δt is:

$$\begin{cases} T_i^* = T_{i-1} - \dfrac{1}{2}\Delta T_{i-1} + \dfrac{W_i \Delta t}{M_i}\dfrac{1}{2}\Delta T_{i-1} & W_i \geq 0 \\ T_i^* = T_i + \dfrac{1}{2}\Delta T_i + \dfrac{W_i \Delta t}{M_{i+1}}\dfrac{1}{2}\Delta T_i & W_i < 0 \end{cases} \tag{18}$$

According to heat transfer experiments of the regenerator conducted by Tew et al. (1978), the heat transfer coefficient between the working fluid and the matrix of the regenerator can be expressed as follows:

$$Nu = 0.06071\,\mathrm{Re} + 3.7 \tag{19}$$

This empirical equation is the linearized testing result from 200×200 *mesh* of the matrix, and is acceptable when applied to the regenerator with similar structure.

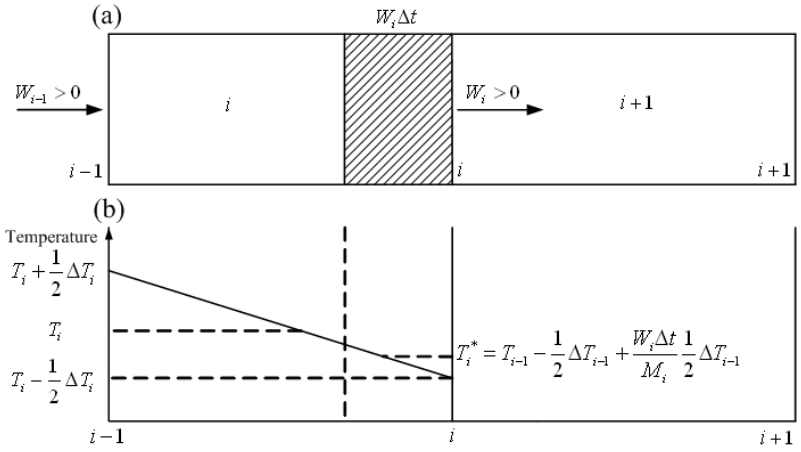

Fig. 3 CVs in the regenerator (a) and temperature distribution (b).

Mechanical loss and auxiliary power

Mechanical loss might occupy a large part of losses in the Stirling engine. The main components of the mechanical losses are in the piston sealing and the guide rings, in the shaft sealing in the exit from the crank-case, in the rolling bearings of the connecting rod big and small ends, in the main crankshaft bearings and in the aerodynamic losses due to the flywheel revolving. Mahkamov (1999) had determined mechanical losses in the construction of the engine, and shown that the mechanical losses for this particular design of the Stirling engine may be up to 50% of the indicated power of the engine. But it is difficult to estimate the mechanical loss of different types of Stirling engine with theoretical equation.

Table 1 Parameters and operational conditions of the P-40 Stirling engine.

Cylinder	Number of cylinder	4
	Stroke	4 *cm*
	Diameter of piston	5.406 *cm*
	Diameter of piston rod	1.2 *cm*
Expansion space	Clearance volume	1.810 *cm*
Compression space	Clearance volume	7.270 *cm*
Regenerator	Number	2
	Porosity of regenerator matrix	0.58
	Dead volume	115.5 cm^3
Cooler	Number	2
	Dead volume	24.13 cm^3
Heater	Number	1
	Dead volume	35.71 cm^3
Operation parameters	Mean pressure	15 *MPa*
	Engine speed	4000 *rpm*
	Average heater wall temperature	993 *K*
	Coolant inlet temperature	323 *K*
	Coolant	Water
	Working fluid	Hydrogen

The common approach is to assume a constant mechanical efficiency in most cases. In this paper, the mechanical loss for the engine is calculated with testing results for the P-40 Stirling engine obtained from NASA (Tew et al., 1978). The P-40 Stirling engine is a portable power generator developed by General Motor for military use (Tew et al., 1978), which is a classical four-cylinder double-acting engine. Detailed geometry parameters and operational conditions of the P-40 Stirling engine are shown in Table 1. NASA Lewis Research Center had provided testing results of the P-40 Stirling engine, variations in the P-40 Stirling engine operating conditions were accomplished by changing the mean pressure and engine speed while remain the temperature of heater wall and coolant unchanged. The working fluid was hydrogen for all P-40 testing cases.

The mechanical loss per engine (4 cylinders) can be written as:

$$W_{ml} = 12.8 \frac{n}{n_d} \frac{p_m + 5}{20} \tag{20}$$

The mechanical loss of P-40 Stirling engine (a four-cylinder double-acting Stirling engine with designed output power of 40 *kW*, which will be used to validate the accuracy of this one-dimensional model) is shown in Fig. 4 with Eq. (20), while Fig. 5 shows the mechanical efficiency of the P-40 Stirling engine over indicated power. We can learn from Fig. 5 that mechanical efficiency decreases with engine speed and increases with mean pressure, and the value of mechanical efficiency for the P-40 Stirling engine could be as low as 70%. However, Eq. (20) is only the testing results for the P-40 Stirling engine, to the other Stirling engines with similar structure, a modified equation can be used to calculate the mechanical loss:

$$W_{ml} = 12.8 \frac{n}{n_d} \frac{p_m + 5}{20} \frac{P_{d,out}}{40} \tag{21}$$

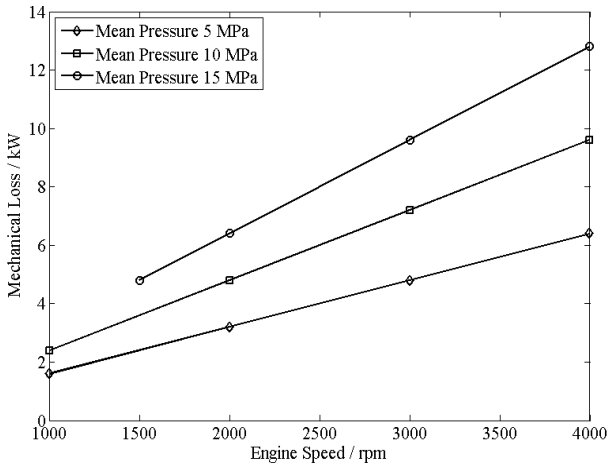

Fig. 4 Mechanical loss of the P-40 Stirling engine as the function of engine speed.

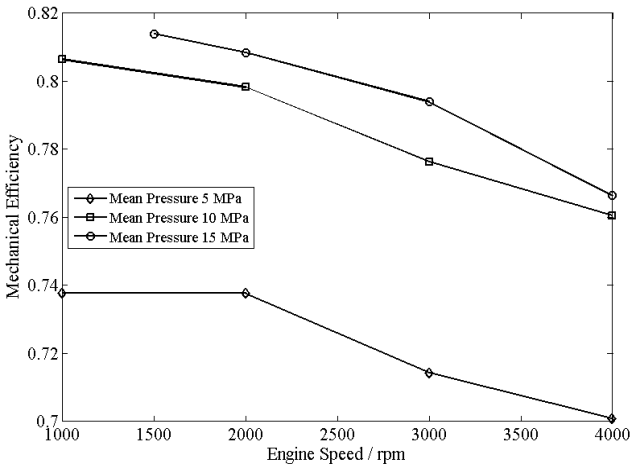

Fig. 5 Mechanical efficiency of the P-40 Stirling engine over indicated power.

In order to operate a Stirling engine effectively and efficiently, a set of auxiliary components should be adopted to support the operation of Stirling engine, thereby consumes a certain amount of output power. These are the power needed to operate the auxiliary machinery such as hydraulics, the vehicle control system and radios, and to operate the payload or sensor equipment in the vehicle. Auxiliary power is also hard to estimate at the design stage and often ignored in this stage. The auxiliary power of the P-40 Stirling engine at the mean pressures of 4 *MPa* and 15 *MPa* is shown in Fig. 6 which is also obtained from testing results conducted by NASA (Tew et al., 1978), and the auxiliary power for mean pressures between 15 *MPa* and 4 *MPa* can be calculated by interpolating this two curves, and the lower curve is defined to be the minimum auxiliary power requirement.

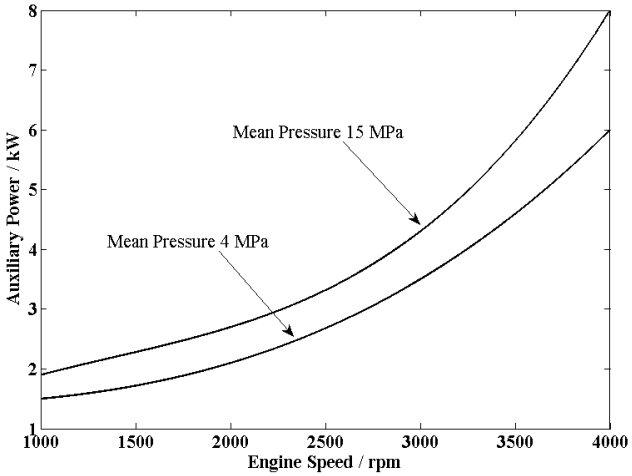

Fig. 6 Auxiliary Power of the P-40 Stirling engine.

Output power

Indicated power P_{in} is written as:

$$P_{in} = \int PdV_c + \int PdV_e \tag{22}$$

Output power is defined as indicated power minus mechanical friction and auxiliary power, which is expressed as:

$$P_{out} = P_{in} - W_{ml} - W_{aux} \tag{23}$$

These equations considered so far have been derived and discussed referring to the generic CV. The aforementioned equations are applied to each CV, thus temperatures, masses, heat transfer coefficients, mass flow rates, etc. are all subscripted with an index for the non-isothermal CVs. The index varies from 1 to Number of CVs (NCV) for variables at CVs and from 1 to ncv-1 for variables defined at the interfaces between CVs, and the grid for the Stirling engine is shown in Fig. 7.

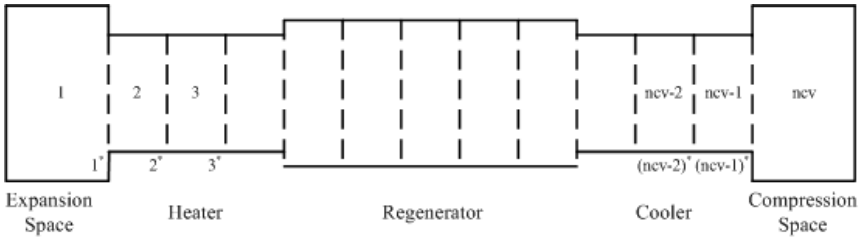

Fig. 7 The grid of the Stirling engine.

RESULTS AND DISCUSSION

Model validation

Validating the one-dimensional model derived, the P-40 Stirling engine from NASA has been used which provided sufficient testing results. Detailed parameters and operational conditions of the P-40 Stirling engine can be found in reference (Tew et al., 1978).

This paper analyses thermodynamic performance of the P-40 Stirling engine under the testing conditions with the one-dimensional model. And, the heater and cooler are divided into 30 CVs, respectively; and the regenerator is divided into 55 grids due to larger temperature gradient.

Fig. 8 shows output power of the P-40 Stirling engine as the function of engine speed at different mean pressures. Output power is under-predicted with the error increasing slightly with increasing engine speed and decreasing slightly with increasing mean pressure, and the maximum error of output power with respect to testing results is less than 18%. Input power in terms of engine speed, for different mean pressures, is shown in Fig. 9, which is under-predicted with the error increasing slightly with increasing engine speed and mean pressure, and the maximum error of input power is no more than 9%. Formosa et al. (Formosa and Despesse, 2010) reviewed comparison results of different numerical models with respect to experiments of the GPU-3 Stirling engine, and the error of indicated power was about 50% for most numerical models. In this way, this one-dimensional model is adequate enough to evaluate the thermodynamic performance of the Stirling engine. To sum up, this one-dimensional model is adequate enough to evaluate the thermodynamic performance of the Stirling engine.

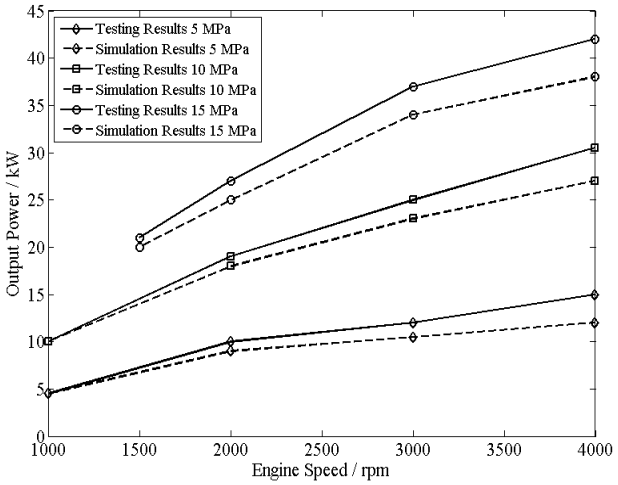

Fig. 8 Output power of the P-40 Stirling engine.

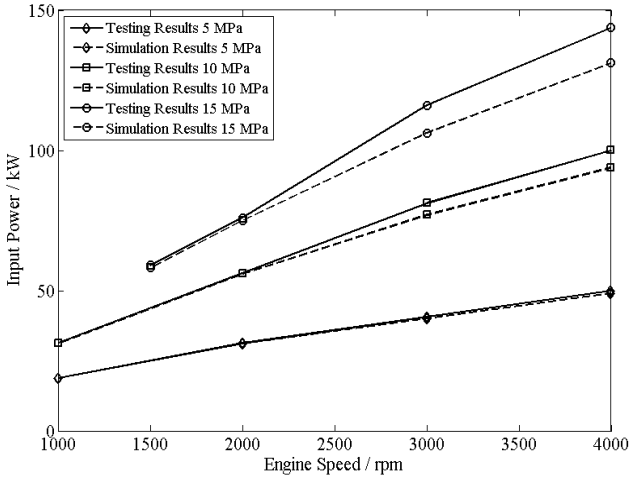

Fig. 9 Iutput power of the P-40 Stirling engine.

Engine design for UUV

As mentioned in the system configuration, the four-cylinder double-acting Stirling engine with output power of 3.5 *kW* is chosen for UUV. For the working fluid, helium rather than hydrogen is selected due to the awareness of safety, even though hydrogen as the working fluid would show a higher thermodynamic performance, and the coolant is sea water with inlet temperature of 293 *K* while assuming the average heater wall temperature is 973 *K* by considering the temperature of wick combustion. The engine speed is chosen as 3600 *rpm* for the design consideration of the propeller for UUV, while the mean pressure is chosen as 12 *MPa*, and mechanical efficiency is assumed as 80% while ignoring auxiliary power.

Table 2 Designed parameters of the Stirling engine for UUV.

Cylinder	Number of cylinder	4
	Stroke	1.65 *cm*
	Diameter of piston	1.85 *cm*
	Diameter of piston rod	0.4 *cm*
Regenerator	Number	4
	Porosity of regenerator matrix	0.7
	Dead volume	2.95 cm^3
Cooler	Number	4
	Dead volume	1.69 cm^3
Heater	Number	4
	Dead volume	4.24 cm^3

A preliminary design of the Stirling engine has been carried out. Shoureshi (Shoureshi, 1978) proposed an optimum design method for the Stirling engine based on simplified Schmidt method, this analytical method could be applied to the optimization of Stirling engine at preliminary stage, this optimum geometry is acquired by minimizing optimum power losses associated with each component over output power. In this paper, the geometry of regenerator, cooler, heater and cylinder are optimized to design a four-cylinder double-acting Stirling engine. Thus, a 3.5kW Stirling engine for UUV with diameter of 21 inches is preliminarily designed, and the designed parameters are tabulated in Table 2. And the showpiece of the designed Stirling Engine system for UUVs is shown in Figs. 10 and 11.

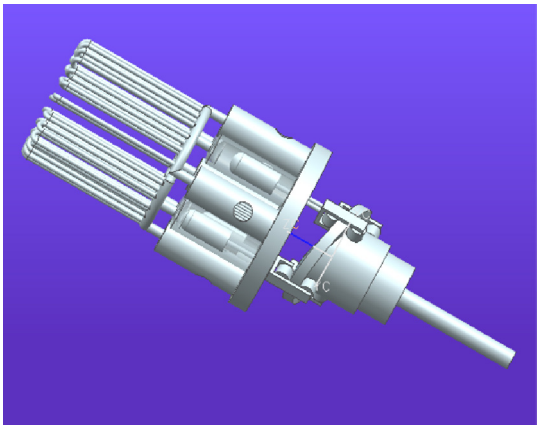

Fig. 10 Stirling engine for UUVs.

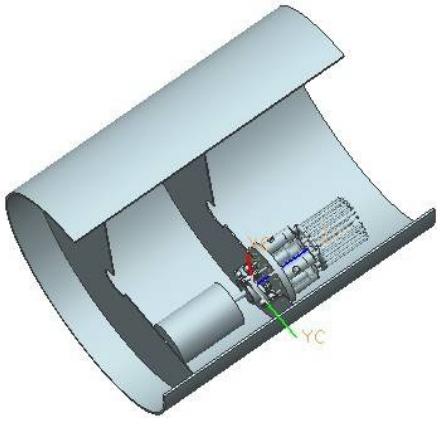

Fig. 11 Stirling engine fixed in UUV with diameter of 21 inches.

However, it is still unknown whether the designed Stirling engine is able to achieve desired output power, then the one-dimensional model is utilized to validate the thermodynamic performance of designed Stirling engine and a comparison of Pressure-Volume (P-V) diagram is shown in Fig. 12 and Fig. 13. The computed value of the output power is 3.28 *kW* and this value is slightly less than the value of 3.5 *kW* which is obtained with the use of Schmidt analysis, because of energy dissipation by mechanical loss or auxiliary power in the modified model. Despite experiments are lacked at this stage to validate the designed parameters, according to the computed results from the one-dimensional model, this designed engine could be capable for outputting 3.5 *kW* power, and further experiments is needed to carry out to study the designed engine.

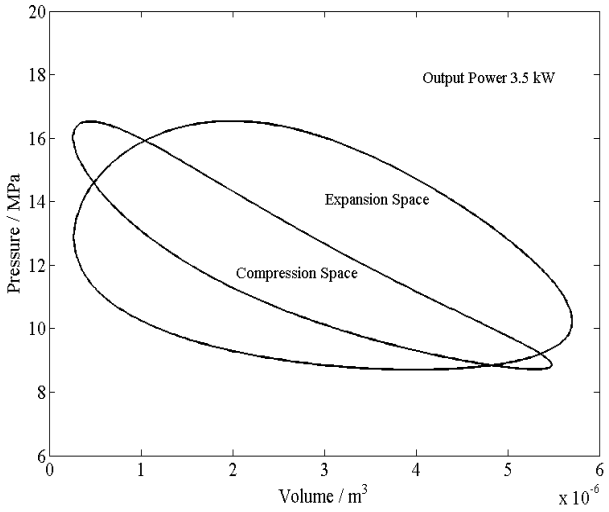

Fig. 12 P-V diagram of the Stirling engine in Schmidt model.

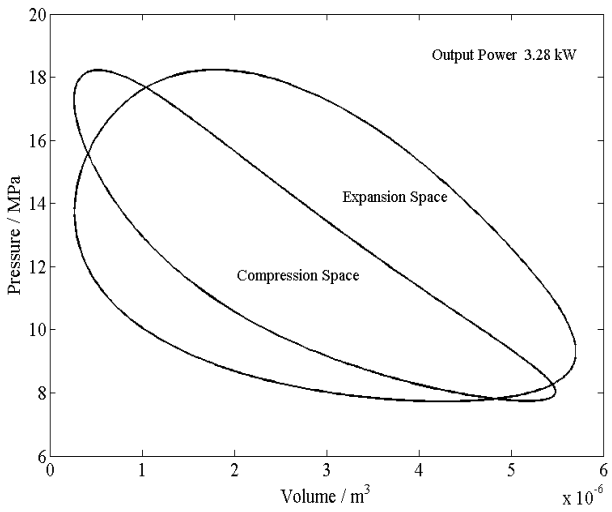

Fig. 13 P-V diagram of the Stirling engine in one-dimensional model.

CONCLUSIONS

In this paper, the configuration of a four-cylinder double-acting Stirling engine is discussed. For the purpose of evaluating the thermodynamic performance of the Stirling engine, a one-dimensional model in which mass conservation, energy conservation and equations of state for real gas are taken as governing equations is derived while referring to NASA Stirling engine computer model, and then modified by combining with mechanical loss and auxiliary power obtained from testing results. The simulation results show that the maximum error of output power of theoretical analysis results is less than 18% over testing results, and the maximum error of input power is no more than 9%.

Furthermore, a 3.5 *kW* Stirling engine is preliminarily designed with Schmidt analysis method, and the one-dimensional model is used to validate the designed engine parameters, the simulation results indicate that this designed engine is capable of showing desired output power. This preliminary study in this paper can provide a certain amount of theory foundation for the development of the Stirling engine for UUV.

ACKNOWLEDGEMENTS

The project is supported by China Scholarship Council, the National Natural Science Foundation of China (NSFC) (Grant No. 51409215) and Natural Science Foundation of Shaanxi Province (Grant No. 2014JQ7263). The authors would like to thank them for the sponsorship.

REFERENCES

Abdullah, S., Yousif, B.F. and Sopian, K., 2005. Design consideration of low temperature differential double-acting Stirling engine for solar application. *Renewable Energy*, 30(12), pp.1923-1941.

Beale, W.T., 1969. Free-Piston Stirling engines-some model tests and simulations. *International Automotive Engineering Congress*, Detroit, Michigan, 13-17 January 1969, pp.1-7.

Bratt, C., 1990. The 4-95 Stirling engine for underwater application. *Proceedings of the 25th Intersociety Energy Conversion Engineering Conference*, Reno, Nevada, USA, 12-17 August 1990, pp.530-533.

Cullen, B. and McGovern, J., 2010. Energy system feasibility study of an Otto cycle/Stirling cycle hybrid automotive engine. *Energy*, 35(2), pp.1017-1023.

Finkelstein, T., 1960. *Generalized thermodynamic analysis of Stirling engine. S.A.E., Paper no. 118B*. New York: SAE.

Formosa, F. and Despesse, G., 2010. Analytical model for Stirling cycle machine design. *Energy Conversion and Management*, 51(10), pp.1855-1863.

Invernizzi, C.M., 2010. Stirling engines using working fluids with strong real gas effects. *Applied Thermal Engineering*, 30 (13), pp.1703-1710.

Kongtragool, B. and Wongwises, S., 2003. A review of solar-powered Stirling engines and low temperature differential Stirling engines. *Renewable and Sustainable Energy Reviews*, 7(2), pp.131-154.

Li, T., Tang, D., Li, Z., Du, J., Zhou, T. and Jia, Y., 2012. Development and test of a Stirling engine driven by waste gases for the micro-CHP system. *Applied Thermal Engineering*, 33-34, pp.119-123.

Mahkamov, K., 1999. Analysis of the working process and mechanical losses in a Stirling engine for a solar power unit. *Journal of Solar Energy Engineering*, 12(2), pp.121-127.

Mahkamov, K., 2006. An axisymmetric computational fluid dynamics approach to the analysis of the working process of a solar Stirling engine. *Journal of Solar Energy Engineering*, 128(1), pp.45-53.

Mancini, T., Heller, P., Butler, B. and Osborn, B., Schiel, W., Goldberg, V., Buck, R., Diver, R., Andraka, C. and Moreno, J., 2003. Dish-Stirling systems: An overview of development and status. *Journal of Solar Energy Engineering*, 125(2), pp.135-151.

Mattavi, J., Heffner, F. and Miklos, A., 1969. *The stirling engine for underwater vehicle applications. SAE Technical Paper 690731*. The city of New York: SAE.

Nilsson, H., 1983. The United Stirling 4-95 and 4-275 Engines for underwater use. *Intersociety Energy Conversion Engineering Conference*, Orlando, FL, USA, 21 August 1983, pp.102-107.

Reader, G., 1988. *Stirling engines: potential applications in marine environment*. U.K.: Institute of Marine Engineers Transactions.

Reader, G., Potter, I.J., Clavelle, E.J. and Fauvel, O.R., 1998. Low power Stirling engine for underwater vehicles applications. *Proceedings of the 1998 International Symposium on Underwater Technology*, Tokyo, Japan, 15-17 April 1998, pp.411-416.

Rogdakis, E.D., Bormpilas, N.A. and Koniakos, I.K., 2004. A thermodynamic study for the optimization of stable operation of free piston Stirling engines. *Energy Conversion and Management*, 45, pp.575-593.

Schmidt, G., 1871. Theorie der Lehmannschen calorischen maschine. *Zeit Des Vereines deutsch Ing*, 15, pp.1-12.

Shih, N.C., Weng, B.J., Lee, J.Y. and Hsiao, Y.C., 2013. Development of a small fuel cell underwater vehicle. *International Journal of Hydrogen Energy*, 38(25), pp.11138-11143.

Shoureshi, R., 1978. *Analysis and design of Stirling engines for waste-heat recovery*. PhD Dissertation. M.I.T.

Tew, R., Jefferies, K. and Miao, D., 1978. *A stirling engine computer model for performance calculations*. Washington *D.C.:* Dept. of Energy, Office of Conservation and Solar Applications, Division of Transportation Energy Conservation.

Timoumi, Y., Tlili, I. and Nasrallah, S.B., 2008a. Design and performance optimization of GPU-3 Stirling engines. *Energy*, 42(33), pp.1100-1114.

Timoumi, Y., Tlili, I. and Nasrallah, S.B., 2008b. Performance optimization of stirling engines. *Renewable Energy*, 42(33), pp.2134-2144.

Tlili, I. and Musmar, S.A., 2013. Thermodynamic evaluation of a second order simulation for Yoke Ross Stirling engine. *Energy Conversion and Management*, 68(4), pp.149-160.

Tlili, I., Timoumi, Y. and Sassi, B.N., 2008. Analysis and design consideration of mean temperature differential Stirling engine for solar application. *Renewable Energy*, 33(8), pp.1911-1921.

Urieli, I. and Berchowitz, D., 1984. *Stirling cycle engine analysis, alternative sources of energy*. Bristol: Adam Hilger.

Wang, X., Shang, J., Luo, Z., Tang, L., Zhang, X. and Li, J., 2012. Reviews of power systems and environmental energy conversion for unmanned underwater vehicles. *Renewable and Sustainable Energy Reviews*, 16(4), pp.1958-1970.

Waters, D.F. and Cadou, C.P., 2013. Modeling a hybrid Rankine-cycle/fuel cell underwater propulsion system based on aluminum-water combustion. *Journal of Power Sources*, 221(1), pp.272-283.